

An ab-initio evaluation of the local effective interactions in the Na_xCoO_2 family

Sylvain Landron,¹ Julien Soret,¹ and Marie-Bernadette Lepetit¹

¹CRISMAT, ENSICAEN-CNRS UMR6508, 6 bd. Maréchal Juin, 14050 Caen, FRANCE

(Dated: May 6, 2019)

We used quantum chemical ab initio methods to determine the effective parameters of Hubbard and $t-J$ models for the Na_xCoO_2 compounds ($x=0$ and 0.5). As for the superconducting compound we found the a_{1g} cobalt orbitals above the e'_g ones by a few hundreds of meV due to the e'_g-e_g hybridization of the cobalt $3d$ orbitals. The correlation strength was found to increase with the sodium content x while the in-plane AFM coupling decreases. The less correlated system was found to be the pure CoO_2 , however it is still strongly correlated and very close to the Mott transition. Indeed we found $U/t \sim 15$, which is the critical value for the Mott transition in a triangular lattice. Finally, one finds the magnetic exchanges in the CoO_2 layers, strongly dependant of the weak local structural distortions.

I. INTRODUCTION

Since the discovery of the large thermoelectric power¹ and then of superconductivity² in the Na_xCoO_2 layered cobaltate family, these systems have attracted a lot of attention. Indeed, they present a very rich phases diagram, as a function of the sodium content x , and the possible water intercalation. For small x ($0 < x < 0.5$) the magnetic susceptibility does not depend on temperature. These systems are thus supposed to be paramagnetic metals, however some authors reinterpreted the data (using NMR measurements³) and conclude that these systems should be antiferromagnetic metals. For larger x ($0.5 < x < 0.75$) the compounds are Curie-Weiss metals. Over $x = 0.75$, the system has been seen as a weakly ferromagnetic metal⁴, however neutron diffraction measurements⁵ rather sees A-type antiferromagnetism, that is ferromagnetic CoO_2 layers, antiferromagnetically coupled. For special values of the sodium content, $x = 1/4$ ⁶, $x = 1/2$ ⁶ and $x = 1$ ⁷, the system is insulating. A band insulator for $x = 1$ and a charge/spin ordered state for $x = 0.5$. On the contrary, for $x = 0$ the system remains conducting⁸⁻¹⁰, exhibiting a Fermi liquid behavior, while its half-filling character associated with the large electron correlation of the cobalt $3d$ let expect a Mott insulator.

The Na_xCoO_2 compounds are composed of CoO_2 layers in the (\vec{a}, \vec{b}) plane, between which the sodium ions are located. The CoO_2 layers are formed by CoO_6 edge-sharing octahedra forming a two-dimensional triangular lattice of cobalt ions. The CoO_6 octahedra present a trigonal distortion along the crystallographic \vec{c} axis corresponding to a compression of the oxygen planes toward the cobalt one. Additional distortions take place, according to the sodium ordering.

In the pure CoO_2 compound, although Tarrascon *et al*¹¹ suggested a complex crystallographic structure, further authors refined the structure with a single cobalt crystallographic position^{8,9}. This system exhibits a geometry quite characteristic compared to the rest of the Na_xCoO_2 family. First, the inter-layer distance is very short. Indeed, the inter-layer distance is 4.48 \AA , 4.31 \AA or 4.25 \AA according to the authors, while for $x \neq 0$ it

ranges from 5.2 \AA to 5.7 \AA and increases with decreasing x . Second, the CoO_2 layer is very compressed in the \vec{c} direction. Indeed, its thickness is only 1.71 \AA while it ranges between 1.92 \AA and 1.98 \AA for the Na_xCoO_2 family. In fact, in this system, the CoO_2 layer is even more compressed than in the superconducting, hydrated compound, for which its thickness is 1.76 \AA . It results in a very large trigonal distortion of the CoO_6 octahedra, with 62.3 degrees between the \vec{c} axis and the Co-O directions. Using the results of reference 12, this strong trigonal distortion lets us expect a strong $a_{1g}-e'_g$ splitting. Third, the Co-O distances are shorter than in all the other compounds of the family, with only 1.847 \AA .

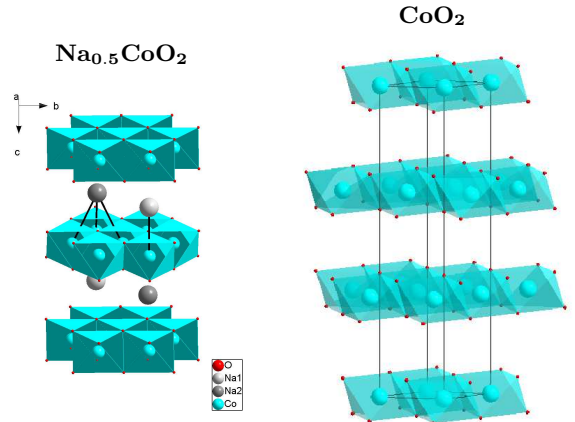


FIG. 1: Schematic structure of the $\text{Na}_{0.5}\text{CoO}_2$ and Na_0CoO_2 compounds. The black lines connect the Na^+ ions with their nearest cobalt neighbors.

In the $\text{Na}_{0.5}\text{CoO}_2$ compound (P2 structure, subject of the present work), the sodiums ordering is commensurate and presents two types of alternated stripes along the \vec{b} direction¹³. In the first stripes, the sodium atoms are located on-top of (below) the cobalts atoms, and in the second type of stripes the sodium ions are located on-top of (below) the center of the cobalt triangles (see figure 1). It results two types of cobalt atoms organized in stripes along the \vec{b} direction, namely the $\text{Co}(1)$ atoms (lo-

cated on top of a sodium ion) and the Co(2) ones. Compared to the other systems of the family, the $\text{Na}_{0.5}\text{CoO}_2$ compound does not stick out¹⁴. Indeed, its CoO_2 layers present a thickness of 1.97 \AA . The average Co–O distances are 1.887 \AA for Co(1) and 1.900 \AA for Co(2). The average trigonal distortions are associated with angles of 58.9 degrees (between the \vec{c} axis and the Co(1)–O directions), and 59.4 degrees (Co(2)–O). These angles are weaker than for the superconducting system or the pure CoO_2 one, but still quite larger than the 54.7 degrees of the regular octahedron. One can thus expect a splitting of the t_{2g} cobalt $3d$ orbitals in two quasi-degenerate e'_g -type orbitals of low energy and a a_{1g} -type one at the Fermi level.

Out of all the Na_xCoO_2 systems, the $x = 0.5$ compound presents a very rich but not well understood phases diagram. Indeed, the Na^+ ions order at very large temperature, namely slightly above 300 K ¹⁵, inducing a small charge order in the cobalt layer. Despite this small charge order the system remains conducting. At 88 K a magnetic phase transition occurs, associated with a structural distortion, and the onset of a long range magnetic order. Again, despite this transition, the system remains conducting up to 53 K where a small charge gap (14 meV) finally opens^{6,16}. The understanding of this complex phase diagram is still under process. Different hypotheses have been advanced such as successive Fermi surface nesting¹⁷, polarons formation¹⁸, one band versus three bands cross-over¹⁹.

As already mentioned, the CoO_2 compound remains conducting for all temperatures, opposite to the Mott insulator behavior that was expected due to its half-filled character. The low temperature dependence of the magnetic susceptibility lead some authors to suggest that this compound is a weakly correlated metal⁹. However, as for the other compounds with $x \leq 0.5$, these data were reinterpreted⁸ in view of NMR measurements as due to strong antiferromagnetic coupling.

In order to understand the low energy physics of these systems it is thus necessary to have accurate determinations of the pertinent degrees of freedom and of their coupling, as a function of the exact crystallographic structure. Indeed, all authors agree on the importance of the sodium ordering and the induced cobalt local environment distortions, on the low energy properties. The aim of this paper is to provide such informations using state of the art quantum chemical spectroscopy methods for the $x = 0.5$ and $x = 0$ compounds. The next section will shortly recall the methods. Section III will presents our results and finally the last section will sum up our conclusions.

II. METHOD AND COMPUTATIONAL DETAILS

A. Ab initio calculations

The method used in this work (CAS+DDCI²⁰) is a configurations interaction method, that is an exact diagonalization method within a selected set of Slater determinants, on embedded crystal fragments. This method has been specifically designed to accurately treat strongly correlated systems, for which there is no single-determinant description. The main point is to treat exactly all correlation effects and exchange effects within a selected set of orbitals (here the $3d$ shell of the cobalt atoms) as well as the excitations responsible for the screening effects on the exchange, repulsion, hopping, etc. integrals.

The CAS+DDCI method has proved very efficient to compute, within experimental accuracy, the local interactions (orbital energies, atomic excitations, exchange and transfer integrals, coulomb repulsion etc.) of a large family of strongly correlated systems such as high T_c copper oxides²¹, vanadium oxides²², nickel and cuprate fluorides²³, spin chains and ladders²⁴, etc.

The clusters used in this work involve one and two cobalt atoms (CoO_6 and Co_2O_{10}) and their oxygen first coordination shell (see figure 2). These fragments are embedded in a bath designed so that to reproduce on them the main effects of the rest of the crystal ; that is the Madelung potential and the exclusion effects of the electrons of the other atoms of the crystal on the clusters electrons.

The electrostatic potential is reproduced by a set of point charges located at the atomic positions. The charges are renormalized next to the bath borders, using the Gellé's method, in order to obtain an exponential convergence of the Madelung potential²⁵. The convergence accuracy was set in the present work to the milli-electron-Volt. The nominal atomic charges used in this work are the formal charges, that is $+3.5$ and $+4$ for the cobalt atoms of the $x = 0.5$ and $x = 0$ compounds, -2 for the oxygen atoms and $+1$ for the sodium atoms. The exclusion effects are treated using total ions pseudo-potentials²⁶ (TIP) on the first shell of atomic sites surrounding the clusters.

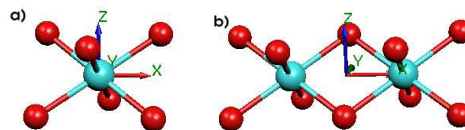


FIG. 2: a) CoO_6 and b) Co_2O_{10} fragments used in the present calculations.

The calculations were done using the MOLCAS²⁷ and CASDI²⁸ suites of programs. The basis sets used can be found in reference 29. The structural parameters were

taken for the $\text{Na}_{0.5}\text{CoO}_2$ system from the 10 K data of reference 13 and for the Na_0CoO_2 system from reference 9.

B. Extracting effective interactions from ab initio results

The results of the ab initio calculations on an embedded fragment of the crystal provide us with energies (E_n) and eigenfunctions (Ψ_n) for the local states from which the crystal ground and low lying excited states are built. Even though these eigenfunctions are expanded over millions of determinants, they are dominated by only few of them, that are usually considered as the implicit basis of the effective models ($t - J$ or Hubbard in the present case). From the effective Hamiltonian theory (for instance such as derived in the quasi-degenerate perturbation theory³⁰) one can extract the main concept necessary to get the effective Hamiltonian parameters from the ab initio results. Indeed, the effective Hamiltonian on the fragment should verify *at the best* the following set of equations

$$H_{\text{eff}}\mathcal{P}\Psi_n = E_n\mathcal{P}\Psi_n \quad (1)$$

where E_n and Ψ_n are the ab initio energies and eigenstates, and \mathcal{P} is the projection operator on the local configurations supporting H_{eff} . For instance, in the present case, these configurations can be the determinants supporting the local singlet and triplet state in the $t - J$ or Hubbard model on the a_{1g} orbitals. The H_{eff} parameters are thus obtained from a mean-square fit minimization of equation 1. These mean-square fit equations can sometime be inverted and the parameters obtained from simple algebraic equations. This is for instance the case for the effective exchange J that is the singlet-triplet excitation energy of a Co_2O_{10} fragment. Similarly, the effective transfer can be simply expressed (see equation 2 in section III C) from the same excitation energy and the knowledge of the wave-functions.

One should however remember that the values of the effective integrals strongly depend on the nature of the effective model. Indeed the processes renormalizing the integrals in one model can be explicit in another and one should take this into account in order to avoid double counting. Let us illustrate our purpose on the t_{2g} orbital energy splitting. In a Hubbard model based on the cobalt $3d$ orbitals the CoO_6 fragment low lying states can be

expressed as

$$\begin{aligned} \Psi_0 &= |e'_{g1}\overline{e'_{g1}}e'_{g2}\overline{e'_{g2}}a_{1g}\rangle \\ \text{with energy} &\quad \varepsilon_{a_{1g}} + 2\varepsilon_{e'_{g1}} + 2\varepsilon_{e'_{g2}} + 2U + 8V - 4J_H \\ \\ \Psi_1 &= |e'_{g1}e'_{g2}\overline{e'_{g2}}a_{1g}\overline{a_{1g}}\rangle \\ \text{with energy} &\quad 2\varepsilon_{a_{1g}} + \varepsilon_{e'_{g1}} + 2\varepsilon_{e'_{g2}} + 2U + 8V - 4J_H \\ \\ \Psi_2 &= |e'_{g1}\overline{e'_{g1}}e'_{g2}a_{1g}\overline{a_{1g}}\rangle \\ \text{with energy} &\quad 2\varepsilon_{a_{1g}} + 2\varepsilon_{e'_{g1}} + \varepsilon_{e'_{g2}} + 2U + 8V - 4J_H \end{aligned}$$

where U is the repulsion of two electrons on the same orbital, V and J_H the repulsion and exchange of two electrons on different $3d$ orbitals. It results that if E_0 , E_1 and E_2 are the ab initio energies associated with these states, the ab initio spectrum should be associated with the orbital energies differences

$$E_1 - E_0 = \varepsilon_{a_{1g}} - \varepsilon_{e'_{g1}} \quad \text{and} \quad E_2 - E_0 = \varepsilon_{a_{1g}} - \varepsilon_{e'_{g2}}$$

On the contrary if one extends the model in order to explicitly treat the differences — according to the nature of the $3d$ orbitals — in the two-electrons two-orbitals repulsion and exchange integrals, then the ab initio spectrum does no more correspond to pure orbital energy differences but rather to

$$\begin{aligned} E_1 - E_0 &= \varepsilon_{a_{1g}} - \varepsilon_{e'_{g1}} + 2(V_{a_{1g}e'_{g2}} - V_{e'_{g1}e'_{g1}}) \\ &\quad - (J_H a_{1g}e'_{g2} - J_H e'_{g1}e'_{g1}) \\ E_2 - E_0 &= \varepsilon_{a_{1g}} - \varepsilon_{e'_{g2}} + 2(V_{a_{1g}e'_{g1}} - V_{e'_{g1}e'_{g1}}) \\ &\quad - (J_H a_{1g}e'_{g1} - J_H e'_{g1}e'_{g1}) \end{aligned}$$

In these equations the two electrons part is non zero as soon as the e'_g orbitals are not pure t_{2g} ones, but rather t_{2g} - e_g hybrids, as it is the case as soon as the trigonal distortion sets in (see reference 12 and section IIIB for the present results). Whether the Racah's parameters are explicitly included in the model or the spherical approximation used, one should thus use different $\varepsilon_{a_{1g}} - \varepsilon_{e'_{gi}}$ effective orbital energy differences in order for the effective Hamiltonian to fit the same ab initio spectrum. In the case of CoO_2 layers it means different ordering for the a_{1g} and e'_g orbitals (see reference 12). As usually done, we will use the spherical approximation in this work and renormalize the orbital energies by the effect of the Racah's parameters.

III. RESULTS

A. On site orbital energy splitting and charge order

A strong controversy has been going on in the literature about the cobalt $3d$ orbital splitting. Indeed, authors did not agree on the relative order of the t_{2g} orbitals

under the trigonal distortion of the regular octahedron ($T_{2g} \rightarrow A_{1g} \oplus E_g$). The origin of the controversy was the fact that the crystalline field theory³¹ as well as some LDA calculations³² found the a_{1g} orbital of lower energy than the e'_g ones, while other density functional calculations³³, as well as quantum chemical calculations³⁴ or ARPES experimental results³⁵ found them of reverse order. We recently showed¹² that the origin of the controversy was an incorrect treatment of the exchange and correlation integrals within the 3d shell. Indeed, only when these effects are taken into account with their whole complexity — that is when the orbital dependence of the two-electron two-orbital on-site repulsion and exchange are correctly treated —, the relative order between the a_{1g} and e'_g orbitals issued from the t_{2g} is correctly predicted. Unfortunately this is not the case in the LDA approximation (essentially due to the local exchange) and thus LDA predicts incorrect a_{1g} - e'_g ordering. This splitting is however one of the crucial parameter for the determination of the nature of Fermi level states as recently shown by Marianetti *et al*³⁶. Indeed, they showed (using DMFT calculations) that the existence of the e'_g pockets in the Fermi surface of the Na_xCoO_2 compounds are directly related to the this splitting. One can thus conclude that the discrepancy between LDA and ARPES Fermi surfaces can be directly related to the improper treatment of the b Racah parameter in LDA. In fact, one can expect that an orbital dependant LDA+U, where the whole complexity of the Racah parameters would be included, should yield Fermi surfaces in agreement with the experimental ones.

We thus computed the t_{2g} orbitals splitting in the two compounds, for the different cobalt sites. These values can be extracted from the spectroscopy of the CoO_6 embedded fragments. Indeed, the excitation energy between the three cobalt states, where one hole is located on one of the t_{2g} orbitals, yield the effective splittings between the a_{1g} and e'_g orbitals. The relative order of the t_{2g} orbitals is displayed on figure 3. One sees immediately

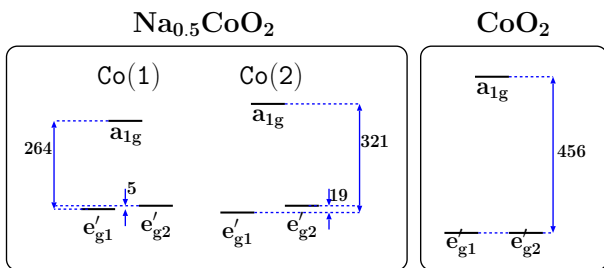


FIG. 3: Schematic representation of the effective cobalt t_{2g} orbital energies in meV. Let us recall that the Co(1) cobalt of the $x = 0.5$ system is located directly under or on top a Na^+ ion.

that the a_{1g} orbitals are always higher than the e'_g ones as can be expected from reference 12. In the $x = 0.5$ system, both sites exhibit a_{1g} orbitals about 250–300 meV higher than the e'_g ones. Similarly, in our dimer calcu-

lations we see that the $\text{Co}^{4+}(1)$ ion is globally of lower energy than the $\text{Co}^{4+}(2)$ ion. Indeed, our calculations yield a global charge order of about 0.17 electrons in favor of the Co(1) site. This result is in agreement with the common sense expectations that will favor a smaller valence for the cobalt with the largest number of Na^+ cations neighbors. Indeed, computing the electrostatic potential difference between the two cobalt sites one finds the Co(1) site about 315 meV lower than the Co(2) site. This result is however in contradiction with the Bond Valence Sum (BVS) model, since the later yields a charge ordering of 0.12 electron in favor of the Co(2) site¹³, however it is in agreement with the LDA+U calculations³⁷ ($\sim 0.16\bar{e}$ in favor of Co(1)). In the pure CoO_2 system, the a_{1g} - e'_g orbital splitting is very large, much larger than in any of the other Na_xCoO_2 systems, even larger than in the superconducting compound. This very large splitting can be easily explained from (i) the large trigonal distortion (the largest observed in this family) and (ii) the very small Co–O distances. Indeed, it was shown in reference 12 that (i) the orbital splitting increases with increasing trigonal distortion and (ii) that the slope of the splitting as a function of the distortion increases linearly with decreasing Co–O distances.

B. Orbital hybridization

Let us now focus on the cobalt 3d orbital hybridization. These orbitals can hybridize in two ways : with the oxygen ligands 2p orbitals, but also within the cobalt 3d shell between the t_{2g} and e_g sets of the regular octahedron. Indeed, it was shown (see ref. 12 for details) that not only this hybridization is symmetry allowed by the trigonal distortion of the octahedron, but also that it is responsible for the lowering of the e'_g orbitals compared to the a_{1g} one. The t_{2g} - e_g hybridization angle is reported in table I and found to be non negligible, of the same order of magnitude as found in the other CoO_2 -based systems. The t_{2g} - e_g hybridization is larger for $x = 0$ than for $x = 0.5$, as can be expected from the larger trigonal distortion.

Orbital	$\text{Na}_{0.5}\text{CoO}_2$		CoO_2
	Co(1)	Co(2)	
e'_{g1}	11.59	11.54	11.86
e'_{g2}	8.21	10.18	11.86

TABLE I: t_{2g} - e_g mixing angle (degrees) in the occupied e'_g cobalt orbitals.

As far as the cobalt ligand hybridization is concerned, we found it to be weak for the a_{1g} and e'_g orbitals, with less than 10% weight on the oxygens. It is however quite large for the empty e_g orbitals with 40 to 45 % weight on the neighboring oxygens.

C. Interatomic interactions

Let us now focus on the interactions between two first neighbor cobalt atoms. Many authors assume that the low energy physics of this compound is determined by the a_{1g} orbitals only. The large $a_{1g}-e'_g$ orbital splitting found in our calculations seem to support this assumption. We thus computed the effective integrals both for a $t-J$ model and a one-band Hubbard model.

Analyzing the low temperature crystallographic structure of $\text{Na}_{0.5}\text{CoO}_2$ (10 K data of reference 13), one sees that there are four types of independent Co–Co bonds (see figure 4), the Co(1)–Co(1) bond, the Co(2)–Co(2) bond and two kinds of Co(1)–Co(2) bonds, namely those where the cobalt–cobalt interactions are mediated by one O(1) and one O(3) oxygen ligands and those where the cobalt–cobalt interactions are mediated by one O(2) and one O(3) oxygen ligands (see figure 4). The effective

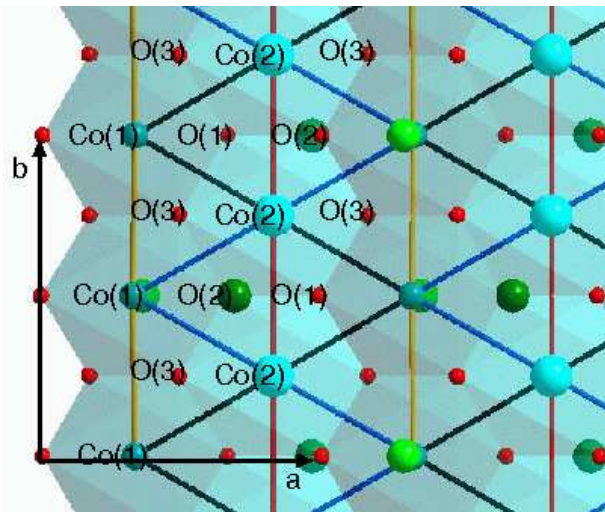


FIG. 4: (color online) Schematic representation of the CoO_2 layers in the $\text{Na}_{0.5}\text{CoO}_2$ compound. There are two different cobalt sites represented in light and darker turquoise color, three different oxygen ligands and the four different Co–Co bonds represented in orange [Co(1)–Co(1)], red [Co(2)–Co(2)], dark blue [Co(1)–Co(2) bridged by O(2) and O(3) oxygens] and black [Co(1)–Co(2) bridged by O(1) and O(3) oxygens].

magnetic exchange integrals are

$$\begin{aligned} J(11) &= -11 \text{ meV} & J(22) &= -27 \text{ meV} \\ J(12^{[13]}) &= -19 \text{ meV} & J(12^{[23]}) &= -19 \text{ meV} \end{aligned}$$

where $J(ij)$ refers to the Co(i)–Co(j) bond and the $[ab]$ superscript refers to the bridging oxygens. For the pure CoO_2 system the magnetic coupling was computed to be much larger with

$$J = -52 \text{ meV}$$

In our notations, the negative integrals correspond to antiferromagnetic coupling. We thus find all exchange inte-

grals, both in the $x = 0$ and $x = 0.5$ compounds, antiferromagnetic, in agreement with the neutron scattering³⁸ and NMR^{8,10} data. One should notice that the exchange integrals are strongly modulated according to the local environment. Indeed, they differ by a factor larger than two for the different bond of the $x = 0.5$ system. It results that this system will be described by a strongly inhomogeneous $t-J$ model. In the $x = 0$ compound the AFM exchange is very large, in agreement with NMR experimental results⁸. The difference in magnitude between the antiferromagnetic coupling of the $x = 0$, $x = 0.5$ and superconducting system³⁴ can easily be explained by the variations in the Co–O distances. Indeed, these distances control for a large part the super-exchange term of the coupling that increases with decreasing distances. It results that following De Vaulx *et al*⁸ we found that AFM fluctuations increase with decreasing x .

Let us now focus on the hopping integrals. One can get them either from the charge fluctuation in the singlet state of the $\text{Co}^{4+}-\text{Co}^{4+}$ fragments, or from the spectroscopy of the $\text{Co}^{3+}-\text{Co}^{4+}$ fragments. A simple analysis shows that the two hopping integrals are somewhat different. In the first case, there is only one spectator electron on the bond, while in the second case, there are two of them (see figure 5). It results in a different eval-



FIG. 5: Schematic representation of the effective hopping integrals as a function of the spectator electrons on the bond. l and r labels refers to the arbitrary “left” and “right” atoms in the fragment.

uation of the hopping integrals according to the number of spectator electrons.

$$\begin{aligned} t(1\bar{e}) &= \langle d_l | h | d_r \rangle + \langle d_l \bar{d}_l | 1/r_{12} | d_r \bar{d}_l \rangle \\ t(2\bar{e}) &= \langle d_l | h | d_r \rangle + \langle d_l \bar{d}_l | 1/r_{12} | d_r \bar{d}_l \rangle + \langle d_l \bar{d}_r | 1/r_{12} | d_r \bar{d}_r \rangle \end{aligned}$$

where the l and r labels refers to the arbitrary “left” and “right” atoms in the fragment, and h is the single electron Hamiltonian part.

$t(1\bar{e})$ can be extracted from the $\text{Co}^{4+}-\text{Co}^{4+}$ fragment. Indeed, mapping a single band Hubbard model on the computed low-energy singlet and triplet states wave functions and energies, one gets after a little algebra

$$t(1\bar{e}) = J \frac{1}{2 \cos \varphi \tan \alpha} \quad (2)$$

$$\bar{U} - V = J \left(1 - \frac{1}{\cos 2\varphi \tan^2 \alpha} \right) \quad (3)$$

assuming the following form for the computed singlet and

triplet wave functions

$$\begin{aligned} \psi_{Sg} = & \cos \alpha \frac{|d_l \bar{d}_r\rangle + |d_r \bar{d}_l\rangle}{\sqrt{2}} \\ & + \sin \alpha \left(\cos \varphi \frac{|d_l \bar{d}_l\rangle + |d_r \bar{d}_r\rangle}{\sqrt{2}} + \sin \varphi \frac{|d_l \bar{d}_l\rangle - |d_r \bar{d}_r\rangle}{\sqrt{2}} \right) \\ & + \text{small terms} \end{aligned}$$

$$\psi_{Tp} = \frac{|d_l \bar{d}_r\rangle - |d_r \bar{d}_l\rangle}{\sqrt{2}} + \text{small terms}$$

$J = E_{Sg} - E_{Tp}$. $\bar{U} - V$ is the effective on-site repulsion of a simple Hubbard model. Let us remind that it accounts for both the average on-site repulsion between the two sites, $\bar{U} = (U_l + U_r)/2$, and the nearest neighbor effective repulsion between the cobalt atoms, $V = V_{lr}$. The (electron-)hopping integrals between the a_{1g} orbitals thus come as

$$\begin{aligned} t_{00}^{1\bar{e}}(11) &= 84 \text{ meV} & t_{00}^{1\bar{e}}(22) &= 139 \text{ meV} \\ t_{00}^{1\bar{e}}(12^{[13]}) &= 115 \text{ meV} & t_{00}^{1\bar{e}}(12^{[23]}) &= 111 \text{ meV} \end{aligned}$$

for the $x = 0.5$ compound and as

$$t_{00}^{1\bar{e}} = 212 \text{ meV}$$

for the $x = 0$ one.

Once again, one sees that the effective transfer integrals are strongly dependant on the local environment of the cobalts and that the $\text{Na}_{0.5}\text{CoO}_2$ system is more inhomogeneous than first thought. In the pure compound, the effective transfer between the a_{1g} orbitals of NN atoms is larger than both in the $x = 0.5$ and the superconducting system. The relative variations of the Co-O and large Co-Co distances between these three systems support the idea that the effective transfer integrals are dominated by the ligand-mediated term rather than the direct hopping term, despite the short metal-metal distances in these edge-sharing compounds.

The transfer integrals with two spectator electrons on the bond, $t^{2\bar{e}}$, can be extracted from the low-energy states of the $\text{Co}^{3+}-\text{Co}^{4+}$ fragments. There are six low energy states according to the localization of the hole on the a_{1g} and e'_g orbitals. The associated effective Hamiltonian can be written as

$$H = \begin{pmatrix} a_{1g}^l & e'_{g1}{}^l & e'_{g2}{}^l & a_{1g}^r & e'_{g1}{}^r & e'_{g2}{}^r \\ \varepsilon_0^l & tp_{10}^l & tp_{20}^l & t_{00}^{2\bar{e}} & t_{10}^{2\bar{e}} & t_{20}^{2\bar{e}} \\ tp_{10}^l & \varepsilon_1^l & tp_{12}^l & t_{10}^{2\bar{e}} & t_{11}^{2\bar{e}} & t_{12}^{2\bar{e}} \\ tp_{20}^l & tp_{12}^l & \varepsilon_2^l & t_{20}^{2\bar{e}} & t_{12}^{2\bar{e}} & t_{22}^{2\bar{e}} \\ t_{00}^{2\bar{e}} & t_{10}^{2\bar{e}} & t_{20}^{2\bar{e}} & \varepsilon_0^r & tp_{10}^r & tp_{20}^r \\ t_{10}^{2\bar{e}} & t_{11}^{2\bar{e}} & t_{12}^{2\bar{e}} & tp_{10}^r & \varepsilon_1^r & tp_{12}^r \\ t_{20}^{2\bar{e}} & t_{12}^{2\bar{e}} & t_{22}^{2\bar{e}} & tp_{20}^r & tp_{12}^r & \varepsilon_2^r \end{pmatrix} \quad (4)$$

where ε_i are the atomic effective orbital energies (see figure 3), $t_{ij}^{2\bar{e}}$ are the effective transfer integrals (direct plus

mediated by the oxygen ligands) between the $3d_i$ orbital of one cobalt and $3d_j$ of the other. tp_{ij} are effective intra-atomic transfer integrals between the d_i and d_j orbitals of the same atom. One may be surprised to find such terms, since the direct integrals are zero due to the Y_l^m symmetry, however the coupling with the bridging oxygen $2p$ orbitals yield in second order perturbation theory an effective intra-atomic transfer term of

$$tp_{ij} = - \sum_p \frac{t_{ip} t_{jp}}{\Delta_p}$$

where i and j refers to the $3d$ orbitals of the same cobalt atom, the sum over p runs over all the ligand bridging orbitals, t_{ip} is the cobalt $3d_i$ -ligand hopping integrals and Δ_p is the excitation energy toward the ligand-to-metal charge transfer configuration. For a more detailed description of the underlying mechanism, one can refer to reference 34. Summing the tp_{ij} contributions coming from the six oxygens around a cobalt atom, one can show that they exactly cancel out in a symmetric system. In the present system, where the atomic S_6 symmetry is not exactly respected, these terms will certainly not exactly cancel out, however, one can expect that their sum will remain very weak.

Table II displays the different effective integrals involved in matrix 4 for the $x = 0.5$ system. One sees

Bond	Inter-atomic transfers (meV)					
	$t_{00}^{2\bar{e}}$	$t_{11}^{2\bar{e}}$	$t_{22}^{2\bar{e}}$	$t_{10}^{2\bar{e}}$	$t_{20}^{2\bar{e}}$	$t_{12}^{2\bar{e}}$
Co(1)-Co(1)	225	-261	-4	-22	-18	-27
Co(2)-Co(2)	281	-325	-11	± 10	-18	± 10

TABLE II: Effective (electron-)hopping integrals between a_{1g} and e'_g orbitals of two neighboring cobalt atoms (in meV).

immediately that the dominant transfer integrals are the inter-atomic hopping between two a_{1g} orbitals and two e'_{g1} orbitals, in agreement with what we found on the superconducting compound. All other integrals are relatively weak ($< 30\text{meV}$) and can probably be omitted in a simple model. Comparing these values with what we found on the superconductor system, one sees that they are of the same order of magnitude, except for the inter-atomic hopping between the a_{1g} orbital of one cobalt and the e'_{g2} orbital of the other. Indeed, the larger value found in the superconducting systems (-53 meV) is now spread over the three $t_{10}^{2\bar{e}}$, $t_{20}^{2\bar{e}}$ and $t_{12}^{2\bar{e}}$ hopping terms, due to local symmetry breaking.

D. On-site repulsion

Let us now examine what we find for on-site the repulsion U from our calculations. Indeed, as detailed in equation 3, the value of $\bar{U} - V$ can be extracted from the singlet and triplet energies and wave functions on the $\text{Co}^{4+}-\text{Co}^{4+}$ fragments. Results for a single band model are presented in table III. One sees immediately that

Compound	$U - V$	$(U - V)/t$
CoO ₂	3.71	15.6
[Na _{0.35} CoO ₂][H ₂ O] _{1.3} ³⁹	3.65	19.4
Na _{0.5} CoO ₂		
$U(1) - V(11)$	2.61	31.1
$U(2) - V(22)$	2.86	20.6
$\overline{U} - V(12^{[13]})$	2.76	24.0
$\overline{U} - V(12^{[23]})$	2.56	23.1

TABLE III: Effective on-site Hubbard repulsion (eV) and correlation strength for different Na_xCoO₂ compounds. $\overline{U} = [U(1) + U(2)]/2$

the Hubbard on-site repulsion decreases with increasing sodium content, that is with increasing number of electrons in the CoO₂ layers. Once again correlating this fact with the Co–O distances one sees that the larger the Co–O distances, the weaker the cobalt on-site repulsion. This can be understood by the fact that a larger volume of the coordination shell around the metal atom will allow its magnetic orbitals to spread over some more and this reduce the intra-orbital repulsion. If one now looks at the correlation strength (U/t) rather than the on-site repulsion value, one sees that the tendency is reverse. Indeed, the larger the sodium content, the larger the correlation strength. It is easy to see that the opposite variation of the correlation strength and the one-site repulsion, as a function of x , is again due to the Co–O distances. Indeed, if an increase of the metal coordination sphere induce a decrease of the effective U , it induces a much stronger reduction of the effective hopping integral t , thus resulting in weaker electronic correlation. This results fit quite well with what was originally supposed (from experimental observations) in these systems, that is a decrease of the correlation strength with x . However it seems hard to say that these systems are weakly correlated, since the smallest U/t ratio is 15.

IV. CONCLUSION

We determined the effective on-site and nearest-neighbor coupling parameters for the the Na_{0.5}CoO₂ and CoO₂ compounds within Hubbard and $t-J$ models. The effective integrals and orbital energies were computed using ab-initio quantum chemical methods treating exactly the strong correlation effects within the cobalt $3d$ shell and the screening effects up to the double-excitations.

The Hubbard on-site repulsion and the correlation strength U/t were found to vary in opposite ways with the sodium content. Indeed, when doping the CoO₂ layer, the t value decreases more rapidly than the U value and the resulting correlation strength increases. For the $x = 0$ limit, however, the system is still strongly correlated with $U/t \sim 15$. This result is in disagreement

with Onoda’s conclusion that the CoO₂ compound is a weakly correlated metal^{9,10}. On the contrary, Julien⁸ concludes the system is a strongly correlated metal close to the Mott phase transition. Our results clearly do agree with the latter hypothesis, indeed, it was shown using DMFT calculation that the Hubbard model reach the Mott transition in a triangular lattice at a critical correlation strength of $U_c/t_c = 15$ ⁴⁰. Our evaluation of the correlation strength : 15.6, clearly situates the CoO₂ compound very close to the Mott transition. Similarly, our results are in agreement with NMR measurements^{8,10} that sees an increase of the antiferromagnetic coupling with decreasing sodium content. However, contrarily to Kawasaki *et al*¹⁰ we do not find the pure CoO₂ compound behaving on a specific way. Indeed, we found it to display the largest antiferromagnetic coupling among all the systems we studied.

We determined the ligand field splitting for the different crystallographically independent cobalts of the Na_{0.5}CoO₂ and CoO₂ compounds. As for the superconducting compound, we find that the a_{1g} orbitals are of higher energy than the e'_g ones, yielding a $e'_g{}^4 a_{1g}{}^1$ cobalt atomic configuration. Comparing the t_{2g} splitting in these two compounds with the splitting in the superconducting compound, we see that it follows the behavior predicted in our previous work¹² both as a function of the amplitude of the trigonal distortion and as the size of the cobalt first coordination shell. Indeed, in the CoO₂ compound, the average distance between the oxygen and cobalt planes is 0.85Å while it is 0.88Å in the superconducting system and ranges between 0.95 and 0.98Å in the $x = 0.5$ compound. As this distance increases with increasing electron doping of the CoO₂ layer, the splitting between the e'_g and a_{1g} orbitals decreases, being maximum for the pure system. Comparing this orbital order with the LDA or LDA+U calculations one sees that it is reverse order. Indeed, tight-binding fitting of the LDA+U calculations yield a higher hole energy by about 0.01eV when located in the a_{1g} orbital⁴¹. Why do LDA calculations yield a reverse order between the a_{1g} and e'_g atomic orbitals than wave-function cluster calculations? The answer is in the treatment of the Coulomb and exchange terms within the 3d shell. Indeed, in LDA calculations the correlation and exchange contributions are treated using a local approximation. It means that the small differences in energy that should occur in these term according to the nature of the occupied 3d orbitals (the b Racah’s parameter) is ignored. This is even worse with LDA+U calculations since the Hartree term is also replaced and a unique U (or rather U , V and J_H) is used while the Coulomb and exchange integrals between two different 3d orbitals depend on the nature of the considered orbitals. These integrals differences are quite small and, in most cases, the averaging is valid enough. In the present case, however, it can be shown that the 2-electron contribution to the orbital energy that is responsible for the a_{1g} - e'_g inversion in reference 12, is a direct function of the Racah’s b integral,

and of the Coulomb and exchange integrals differences. The effects of these imperfect exchange and correlation treatment within the 3d shell, and thus of the resulting orbital order between the a_{1g} and e'_g orbitals is to pop up the band issued from the later in comparison with the bands issued from the former. Indeed, it was shown by Marianetti *et al*³⁶ (using DMFT calculations) that when the a_{1g} orbital is supposed of higher energy (lower hole energy) than the e'_g orbital, the e'_g pockets in the Fermi surface disappear. More recently Bourgeois *et al*⁴² showed that using orbital splitting of the same sign and order of magnitude as in the present work, DMFT Fermi surfaces and band structure nicely fit the ARPES data (they studied different systems ranging from $x = 0.3$ to $x = 0.7$). In view of our results and the above analysis we think that the e'_g Fermi pockets found in LDA calculations and not observed in ARPES experiments are due to an intrinsic feature of the LDA exchange and correlation functional and thus that these pockets are true artefacts of the method.

Finally, one should remember the strong variation of the effective exchange and hopping integrals as a function of the local distortions. This fact can be of importance in the understanding of the changes in magnetic behavior, as a function of x , in the Na_xCoO_2 family. It would thus be of interest to see if the local distortions observed for larger x values will be able to reverse the sign of the magnetic exchange as suggested by neutron diffraction experiments.

Acknowledgments

The authors thank Daniel Maynau for providing us with the CASDI suite of programs. These calculations were done using the CNRS IDRIS computational facilities under project n°1842 and the CRIHAN computational facilities under project n°2007013.

-
- ¹ I. Terasaki, Y. Sasago and K. Uchinokura, Phys. Rev. **B 56**, R12685 (1997) ; W. Koshibae, K. Tsutsui and S. Maekawa, Phys. Rev. **B 62**, 6869 (2000).
- ² K. Takada, H. Sakurai, E. Takayama-Muromachi, F. Izumi, R. A. Dilanian and T. Sasali, Nature **422**, 53 (2003).
- ³ G. Lang, J. Bobroff, H. Alloul, G. Collin and N. Blanchard, Phys. Rev. **B 78**, 155116 (2008).
- ⁴ M. L. Foo, Y. Wang, S. Watauchi, H.W. Zandbergen, T. He, R.J. Cava and N.P. Ong, Phys. Rev. Letters **92**, 247001 (2004).
- ⁵ S. P. Bayracki, I. Mirebeau, P. Bourges, Y. Sidis, M. Enderle, J. Mesot, D. P. Chen, C. T. Lin, B. Keimer, Phys. Rev. Lett. **94**, 157205 (2005) ; L. M. Helme, A. T. Boothroyd, R. Coldea, D. Prabhakaran, D. A. Tennant, A. Hiess, and J. Kolda, Phys. Rev. Lett. **94**, 157206 (2005).
- ⁶ J. Hwang, J. Yang, T. Timusk and F. C. Chou, Phys. Rev. **B 72**, 024549 (2005).
- ⁷ C. de Vaulx, M.-H. Julien, C. Berthier, M. Horvatić, P. Bordet, V. Simonet, D. P. Chen and C. T. Lin, Phys. Rev. Letters **95**, 186405 (2005).
- ⁸ C. De Vaulx, M.-H. Julien, C. Berthier, S. Hbert, V. Pralong and A. Maignan, Phys. Rev. Lett. **98**, 246402 (2007).
- ⁹ M. Onoda and A. Sugawara, J. Phys: Cond. Matter **20**, 175207 (2008).
- ¹⁰ S. Kawasaki, T. Motohashi, K. Shimada, T. ono, R. Kanno, M. Karppinen, H. Yamauchia and Guo-qing Zheng, Phys. Rev. **B 79**, 220514R (2009).
- ¹¹ L. Seguin, G. Amatucci, M. Anne, Y. Chabre, P. Ströbel, J.-M. Tarrascon and G. Vaughan, J. Power Sources **81-82**, 604 (1999).
- ¹² S. Landron and MB Lepetit, Phys. Rev. **B 77**, 125106 (2008).
- ¹³ A. J. Williams, P. J. Atfield, M. L. Foo, L. Viciu and R. J. Cava, Phys. Rev **B 73**, 134401 (2006).
- ¹⁴ L. Viciu, J. W. G. Bos, H. W. Zandbergen, Q. Huang, M. L. Foo, S. Ishiwata, A. P. Ramirez, M. Lee, N. P. Ong and R. J. Cava, Phys. Rev. **B 73**, 174104 (2006).
- ¹⁵ D. N. Argyriou, O. Prokhnenko, K. Kiefer and C. J. Milne, Phys. Rev. **B 76**, 134506 (2007).
- ¹⁶ P. Mendels, D. Bono, J. Bobroff, G. Collin, D. Colson, N. Blanchard, H. Alloul, I. Mukhamedshin, F. bert, A. Amato and A. D. Hillier, Phys. Rev. Lett. **14**, 136403 (2005).
- ¹⁷ J. Bobroff, G. Lang, H. Alloul, N. Blanchard and G. Collin, Phys. Rev. Lett. **96**, 107201 (2006).
- ¹⁸ N. L. Wang, Dong Wu, G. Li, X. H. Chen, C. H. Wang and X. G. Luo, Phys. Rev Lett. **93**, 147403 (2004).
- ¹⁹ K. W. Lee, J. Kuneš and W. E. Pickett, Phys. Rev. **B 70**, 045104 (2004).
- ²⁰ J. Miralles, J. P. Daudey and R. Caballol, Chem. Phys. Lett. **198**, 555 (1992) ; V. M. García *et al.*, Chem. Phys. Lett. **238**, 222 (1995) ; V. M. García, M. Reguero and R. Caballol, Theor. Chem. Acc. **98**, 50 (1997).
- ²¹ D. Muñoz, F. Illas and I. de P.R. Moreira, Phys. Rev. Letters **84**, 1579 (2000) ; D. Muñoz, I. de P.R. Moreira and F. Illas, Phys. Rev.**B 65**, 224521 (2002).
- ²² N. Suaud and M.-B. Lepetit, Phys. Rev. **B 62** 402 (2000) ; N. Suaud and M.-B. Lepetit, Phys. Rev. Letters **88**, 056405 (2002).
- ²³ I. de P.R. Moreira, F. Illas, C. Calzado, J.F. Sanz J.-P. Malrieu, N. Ben Amor and D. Maynau, Phys. Rev. **B59**, R6593 (1999).
- ²⁴ A. Gellé and M.B. Lepetit, Phys. Rev. Letters **92**, 236402 (2004) ; A. Gellé and M.B. Lepetit, Eur. Phys. J. **B 43**, 29 (2005) ; Alain and M.B. Lepetit, Eur. Phys. J. **B 46**, 489 (2005).
- ²⁵ A. Gellé and M.B. Lepetit, J. Chem. Phys. **128**, 244716 (2008).
- ²⁶ N. W. Winter, R. M. Pitzer and D. K. Temple, *J. Chem. Phys.* **86**, 3549 (1987).
- ²⁷ G. Karlström, R. Lindh, P.-Å. Malmqvist, B. O. Roos, U. Ryde, V. Veryazov, P.-O. Widmark, M. Cossi, B. Schimmelpfennig, P. Neogrady, L. Seijo, Computational Material Science **28**, 222 (2003).
- ²⁸ D. Maynau *et al*, CASDI suite of programs kindly provided

- by D. Maynau.
- ²⁹ Z. Barandiaran and L. Seijo, *Can. J. Chem.* **70**, 409 (1992).
- ³⁰ See for instance chapter 9.4 in *Atomic Many-Body Theory*, I. Lindgren and J. Morrison, Springer, Berlin (1982).
- ³¹ W. Koshibae and S. Maekawa, *Phys. Rev. Letters* **91**, 257003 (2003).
- ³² M. D. Johannes, I. I. Mazin, D. J. Singh and D. A. Papaconstantopoulos, *Phys. Rev. Letters* **93**, 9 (2004).
- ³³ L.-J. Zou, J.-L. wang and Z. Zeng, *Phys. Rev. B* **69**, 132505 (2004).
- ³⁴ S. Landron and MB Lepetit, *Phys. Rev B* **74** 184507 (2006).
- ³⁵ H.-B. Yang, Z.-H. Pan A. K. P. Sekharan, T. sato, S. Souma, T. Takahashi, R. Jin, B. C. Sales, D. Mandrus, A. D. Ferorov, Z. Wang and H. Ding, *Phys. Rev. Lett.* **95**, 146401 (2005).
- ³⁶ C.A. Marianetti, K. Haule and O. Parcolet, *Phys. Rev. Lett.* **99**, 246404 (2007).
- ³⁷ K.-W. Lee, J. Kuneš, P. Novak and W. E. Pickett, *Phys. Rev. Lett.* **94**, 026403 (2005).
- ³⁸ G. Gašparović, R. A. Ott, J.-H. Cho, F. C. Chou, Y. Chu, J.W. Lynn and Y. S. Lee, *Phys. Rev. Lett* **96**, 046403 (2006).
- ³⁹ S. Landron, PhD. Thesis, Université Paul Sabatier, Toulouse (France).
- ⁴⁰ J. Merino, B. J. Powell and R. H. McKenzie, *Phys. Rev. B* **73**, 235107 (2006).
- ⁴¹ S. Zhou, M. Gao, H. Ding, P. A. Lee and Z. Wang, *Phys. Rev. Letters* **94**, 206401 (2005).
- ⁴² A. Bourgeois, A. A. Aligia and M. J. Rozenberg, *Phys. Rev. Letters* **102**, 066402 (2009).